Large-Eddy Simulations of Baroclinic Instability and Turbulent Mixing

Eric D. Skyllingstad
College of Oceanic and Atmospheric Sciences, Oregon State University
104 COAS Admin. Bldg.
Corvallis, OR 97331
Phone: (541) 737-5697 Fax: (541) 737-2064 Email: skylling@coas.oregonstate.edu

Roger M. Samelson
College of Oceanic and Atmospheric Sciences, Oregon State University
104 COAS Admin. Bldg.
Corvallis, OR 97331
Phone: (541) 737-4752 Fax: (541) 737-2064 Email: rsamelson@coas.oregonstate.edu

Award Number: N00014-09-1-0268

LONG-TERM GOAL

The long-term goal of this project is to improve our ability to understand, model and predict lateral mixing and the associated submesoscale physical structure and processes in the upper and interior ocean.

OBJECTIVES

The main objective of this project is to examine the interaction between baroclinic, mesoscale eddies and turbulence using a large-eddy simulation (LES) model. Cases will focus on strong, baroclinic waves that form in the mixed layer along surface fronts with scales of a few km, and on mesoscale eddies that are imbedded within larger scale frontal regions. Our goal is to quantify, understand, and ultimately parameterize the physical processes that lead to lateral mixing. Simulations will help guide field experiments planned as part of the Lateral Mixing DRI, and provide a tool for understanding observations in the analysis phase of the project.

APPROACH

High-resolution simulations of baroclinic instability and the interaction of mesoscale flow with turbulent mixing are conducted and analyzed using a large-eddy simulation model. Our analysis centers on quantifying and understanding the mechanisms by which small-scale turbulent structure develops on the mesoscale field, the physical processes and balances that control lateral mixing of fluid properties across the unstable front, and the transition from strongly horizontal, geostrophic motion on the mesoscale to three-dimensional, quasi-isotropic, non-hydrostatic motion on turbulent scales.

Report Documentation Page

Form Approved
OMB No. 0704-0188

1. REPORT DATE **30 SEP 2011**	2. REPORT TYPE	3. DATES COVERED **00-00-2011 to 00-00-2011**

4. TITLE AND SUBTITLE **Large-Eddy Simulations of Baroclinic Instability and Turbulent Mixing**	5a. CONTRACT NUMBER
	5b. GRANT NUMBER
	5c. PROGRAM ELEMENT NUMBER
6. AUTHOR(S)	5d. PROJECT NUMBER
	5e. TASK NUMBER
	5f. WORK UNIT NUMBER
7. PERFORMING ORGANIZATION NAME(S) AND ADDRESS(ES) **Oregon State University,College of Oceanic and Atmospheric Sciences,104 COAS Admin. Bldg,Corvallis,OR,97331**	8. PERFORMING ORGANIZATION REPORT NUMBER
9. SPONSORING/MONITORING AGENCY NAME(S) AND ADDRESS(ES)	10. SPONSOR/MONITOR’S ACRONYM(S)
	11. SPONSOR/MONITOR’S REPORT NUMBER(S)

12. DISTRIBUTION/AVAILABILITY STATEMENT
Approved for public release; distribution unlimited

13. SUPPLEMENTARY NOTES

14. ABSTRACT

15. SUBJECT TERMS

16. SECURITY CLASSIFICATION OF:			17. LIMITATION OF ABSTRACT	18. NUMBER OF PAGES	19a. NAME OF RESPONSIBLE PERSON
a. REPORT **unclassified**	b. ABSTRACT **unclassified**	c. THIS PAGE **unclassified**	**Same as Report (SAR)**	**6**	

WORK COMPLETED

Research during the third year of this project has focused on analyzing the effects of baroclinic instability on lateral mixing with emphasis on determining how energy is transferred between baroclinic disturbances and three-dimensional turbulence. Work also has focused on understanding how boundary layer turbulence affects dispersion of dye and the role of shear dispersion versus mixing by Langmuir circulation.

RESULTS

Baroclinic Instability

Simulations of baroclinic instability are conducted using a large-eddy simulation model for a dual frontal system representing a warm pool contained within a periodic domain. Two symmetric fronts are initialized within an 80 m deep mixed layer and evolve over a period of 4-5 days as shown in Figure 1.

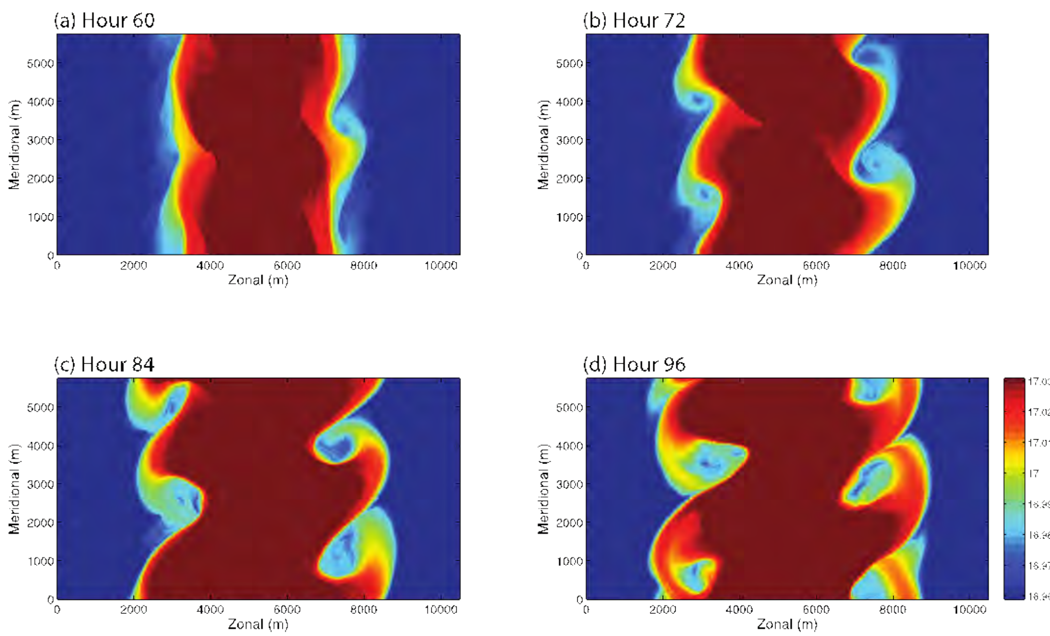

Figure 1. Horizontal sections of temperature (°C) taken at hour (a) 60, (b) 72, (c) 84, and (d) 96 from a depth of 4.5 m for a simulation with no surface forcing.

Analysis of the kinetic energy budget provides a perspective on the transfer of energy across scales in the simulation. We first examine the time evolution of the perturbation kinetic energy by calculating the averaged budget,

$$\frac{\partial e}{\partial t} = u_i' \cdot \frac{\partial u_i}{\partial t} = u_i' \cdot u_i \nabla u_i + u_i' \cdot \nabla p - u_3' \delta_{i3} g \frac{\rho'}{\rho_o} - u_i' \cdot \frac{\partial \left(\overline{u_i'' u_j''}\right)}{\partial x_i} \qquad (1)$$

I II III IV V

where

$$u_i'(x,y,z,t)=u_i(x,y,z,t)-U_i(x,z,t), \quad U_i(x,z,t)=\frac{1}{y_{\max}}\sum_{y=0}^{y=y_{\max}} u_i(x,y,z,t).$$

The terms in (1) are referred to here as (I) storage, (II) shear production, (III) pressure work, (IV) buoyancy production, and (V) dissipation. Average velocity fields are calculated as meridional means and approximately represent the geostrophic background flow that is initially in thermal wind balance. The full-domain integral of (I) in (1) is then equal to the rate of change of the domain-integral of the fluctuation kinetic energy, .

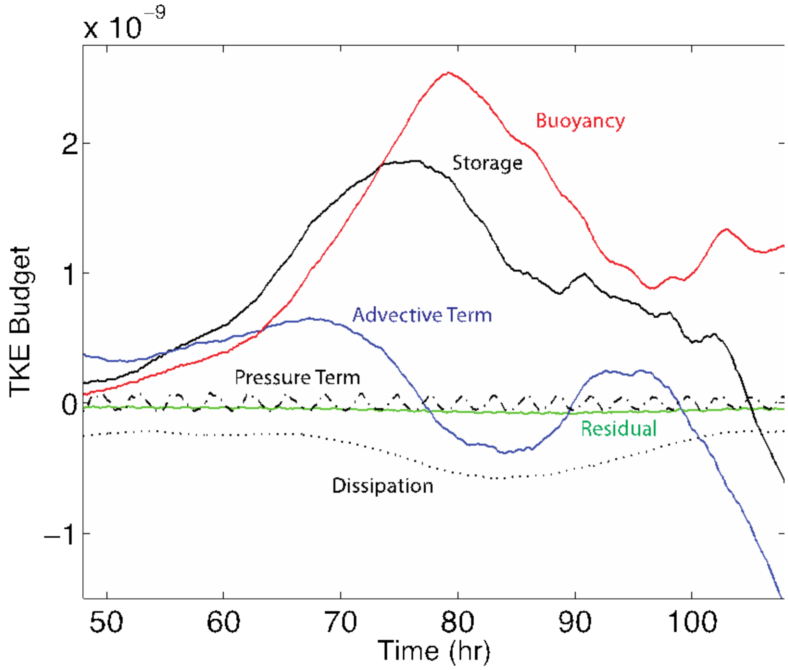

Figure 2. Domain averaged kinetic energy budget terms ($m^2\ s^{-3}$) as a function of time for the simulation in Figure 1. Terms are I-V as defined in the text and are labeled here as I – Storage, II – Advective Term, III – Pressure Term, IV – Buoyancy, V – Dissipation, with Residual equal to the sum of I-V.

Energy production in the model is dominated by the buoyancy term (I), representing the release of available potential energy from the horizontal density gradients of the large-scale flow (Figure 2). The positive storage term represents the increasing kinetic energy of the growing baroclinic waves. The shear production term represents conversion of mean kinetic energy to perturbation kinetic energy through horizontal shear production. Initially, this term is positive, indicating that the instability is of mixed baroclinic-barotropic type. As the disturbances amplify, this term reverses sign, suppressing the wave growth as the waves occlude around hour 78 (Fig. 2), after which time wave growth decreases rapidly with formation of ring circulations by hour 96. This transition reflects the classical progression of a baroclinic life-cycle from baroclinic, or mixed baroclinic-barotropic, growth to barotropic decay (e.g., Simmons and Hoskins, 1978; Samelson and Chapman, 1995). Dissipation is always negative, but through most of the simulation is much smaller than the buoyancy forcing, indicating that the baroclinic modes are not transferring significant amounts of energy to small-scale motions. The pressure work term has a small oscillation associated with pseudo-compressibility of the iterative

numerical solver; when averaged over the oscillation period, this term is negligibly small, as required for an unforced incompressible fluid in a periodic domain with a rigid top and bottom.

Vertical profiles of horizontal averages of the instantaneous balance (7) at hour 72 show that the buoyancy production (I) is a large generation term through the middle of the mixed layer, with shear production (II) adding energy except near the surface and near the mixed layer bottom. Dissipation is relatively weak throughout the entire column with a maximum near the surface where small-scale eddies have the largest amplitude (e.g. figure 1). Pressure work primarily acts to redistribute energy away from the middle of the mixed layer and counteracts shear production near the surface.

A key question in our analysis concerns the fate of kinetic energy generated at baroclinic scales, which can be removed from the system by either altering the density structure of the background (e.g. frontal slumping or restratification) or through explicit and sub-grid-scale viscous dissipation. The structure of kinetic energy spectra as a function of horizontal wave number magnitude $k = (k_x + k_y)^{1/2}$ for the current simulation (from a two-dimensional spectral decomposition, averaged over wavenumber vectors of approximately equal magnitude, and then divided by k to obtain the spectral density) suggest that energy at large scales is not effectively moving downscale, as the spectral slope is about -3, more indicative of an energy-conserving enstrophy-cascade than an energy-cascade regime. This is consistent with the integrated energy budget (Fig. 2), showing that the dominant energy balance is inviscid. There is enhanced energy and shallower spectral slope at the largest wavenumbers, very near the model resolution.

Dye Dispersion

A second area of research that we are investigating concerns the dispersion of dye by mixing in the ocean surface boundary layer. Observations of dye taken from aircraft in preliminary experiments leading up to Latmix suggest that dye patches are capable of outlining mixing circulations contained in the ocean boundary layer. An example is presented in figure 3 taken from field data off the coast of Florida. Lateral banding in the dye observations suggests that circulations in the mixed layer are actively concentrating the dye along the wind direction, which was from the northwest at the time of the experiment.

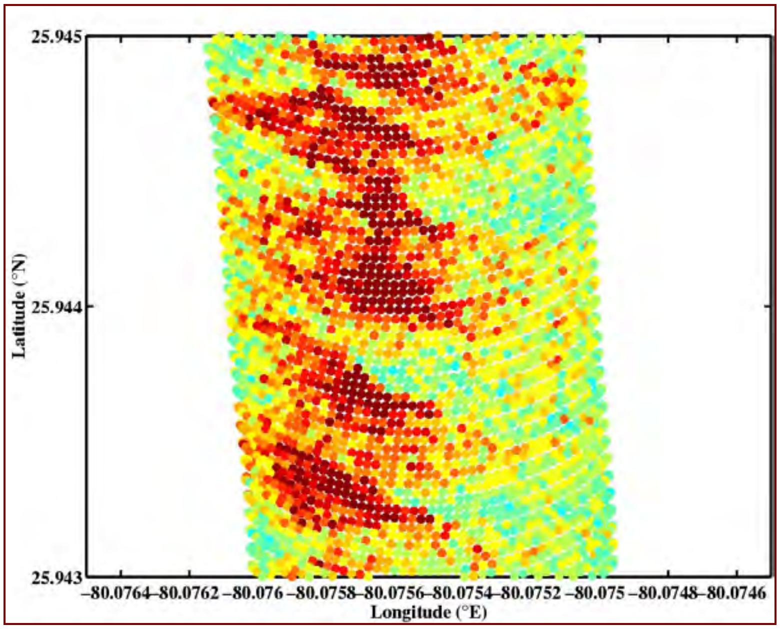

Figure 3. Rhodamine dye streak observations taken from aircraft off the coast of Florida in 2004.

Banding of the dye could be produced by either roll vortices forced by shear instability or by Langmuir circulation produced by surface waves. Further insight into this question can be obtained by simulating the behavior of dye using a large eddy simulation model with and without wave forcing. Simulations with equivalent wind stress forcing but different surface wave conditions are shown in Figure 4. Here, the wave forcing is based on the Craik and Leibovich (1976) vortex force and leads to a significant reduction in mixed layer shear in comparison with the case with no wave effects (Fig. 4b). Without waves, shear dispersion stretches the simulated dye plume over scales roughly 2 times the wave-forced case.

Based on these experiments, we conclude that dye experiments should provide a means for determining the importance of Langmuir circulation in typical wind and wave forced seas. If the vortex force is not active, then we would expect a much higher rate of lateral dispersion in comparison with situations with active Langmuir turbulence. Analysis of observed dye cases taken during the East Coast LatMix experiment is underway to determine if the rate of dispersion is consistent with reduced shear accompanying Langmuir circulation.

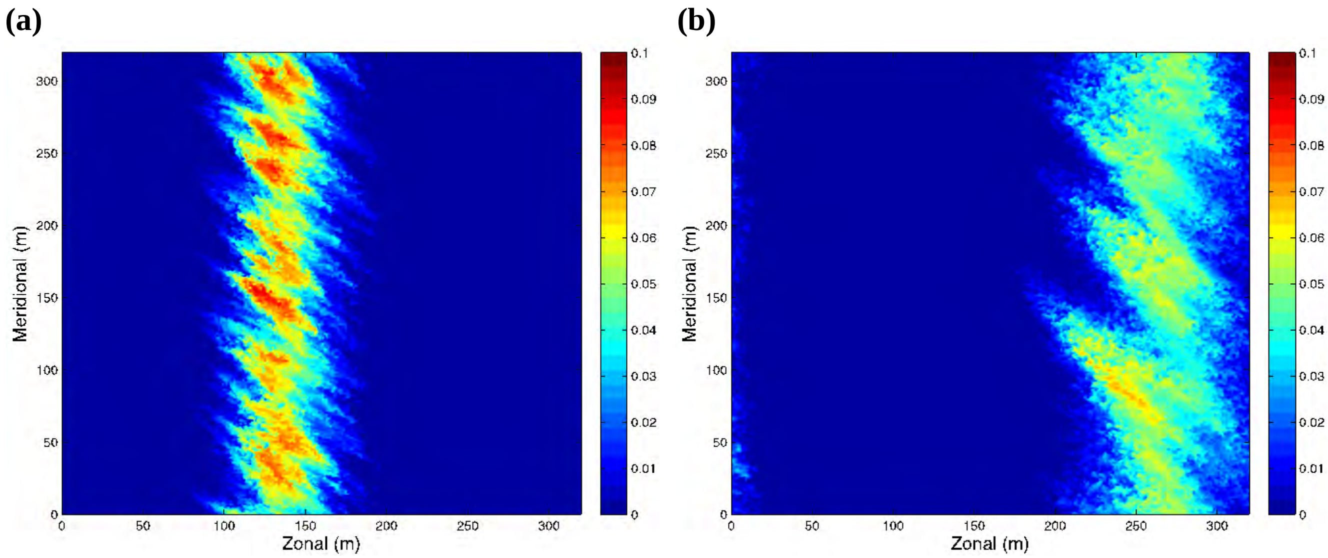

Figure 4. Simulated dye dispersion (a) with wave forcing and (b) without wave forcing.

RELATED PROJECTS

This project is part of the ONR Lateral Mixing Directed Research Initiative (DRI) and is related to other modeling and field projects supported under that DRI.

REFERENCES

Craik, A. D. D., and S. Leibovich, 1976. A rational model for Langmuir circulations. *J. Fluid Mech.*, 73, 401-426.

Samelson, R. M., and D. C. Chapman, 1995: Evolution of the instability of a mixed-layer front. *Journal of Geophysical Research*, 100(C4), 6743-6759.

Simmons, A. J., and B. J. Hoskins, 1978: Barotropic influences on the growth and decay of some non-linear baroclinic waves. *J. Atmos. Sci.*, 37, 1679-1684.

PUBLICATIONS

Skyllingstad, E. D. and R. M. Samelson, 2011. Baroclinic Frontal Instabilities and Turbulent Mixing in the Surface Boundary Layer. Part I: Unforced, J. Phys. Oceanogr., submitted.